Journal of Alloys and Compounds, 213/214 (1994) 138–147
JALCOM 4007

Electronic structure properties of neptunium intermetallics under pressure from Mössbauer spectroscopy

G.M. Kalvius and W. Potzel
Physics Department, Technical University Munich, D-85747 Garching (Germany)

S. Zwirner
Physics Department, Technical University Munich, D-85747 Garching (Germany)
and European Institute for Transuranium Elements, D-76125 Karlsruhe (Germany)

J. Gal
Physics Department, Technical University Munich, D-85747 Garching (Germany)
and Department of Nuclear Engineering, Ben Gurion University of the Negev, 84120 Beer Sheva (Israel)

I. Nowik
Racah Institute of Physics, The Hebrew University, 91904 Jerusalem (Israel)

Abstract

Electronic structure properties of neptunium intermetallics obtained by the 60 keV Mössbauer resonance in ^{237}Np in the pressure range up to 9 GPa and at temperatures from 1.5 K to about 150 K together with X-ray determinations of the bulk modulus are discussed. Samples of the NaCl compounds NpX, the Laves phases NpX_2 and the $AuCu_3$ materials NpX_3 as well as the tetragonal series NpX_2Si_2 have been studied. The volume coefficients of magnetic moment and magnetic transition temperature allow the classification in terms of 5f bandwidth arising either from 5f–5f overlap or hybridization with ligand s, p, or d electrons. The pressure–temperature magnetic phase diagram of some of these compounds has also been investigated. In $NpGa_3$ and $NpIn_3$ we find a preference for ferromagnetic order under reduced volume. Finally we address the question of crystal field interactions and show that even in a somewhat delocalized case ($NpAl_2$) they are decisive in determining the high pressure Mössbauer spectra.

1. Introduction

The basis of what will be discussed in this paper dates back to several contributions presented at the ancestor of modern actinide conferences here in Santa Fe 23 years ago [1]. Firstly, the strong correlation between magnetic properties and separation of neighbouring actinide ions was pointed out by Hill [2]. Secondly, relativistic band structure calculations (mainly for the elemental metals) showed that the 5f electrons indeed form band-like states and that 5f–5f overlap is here the important mechanism for delocalization of 5f electrons [3]. Thirdly, another theoretical paper dealt with crystalline field effects in cubic actinide compounds [4]. Fourthly, Mössbauer spectroscopy in Np, first successfully demonstrated by Stone and Pillinger [5] in 1964, had come of age and presented itself as an important tool to gain insight into electronic structure properties, especially magnetic behaviour, of Np compounds [6]. Mössbauer spectroscopy on Np has been and is the spearhead for studies in solid state physics and chemistry of metallic and non-conducting compounds mainly because neither impurities nor sample encapsulation interferes directly with the measurements and that only rather small amounts of polycrystalline powder material are needed. Reviews of the results obtained have appeared over the years, more recently in refs. 7 and 8.

The obvious goal to combine Np Mössbauer spectroscopy with the application of pressures high enough to induce volume reductions of the order of some per cent needed another decade of technical development [9]. Until now, progress in this field has been slow and our group at the Technical University, Munich, is unfortunately still the only group performing this type of measurement. Special emphasis has recently been placed on materials with the $AuCu_3$ structure. One of the major disadvantages in interpreting high pressure data quantitatively is that band structure calculations with atomic volume as a variable are close to non-

SSDI 0925-8388(93)04007-D

existent. It is our sincere hope that this unfortunate situation will improve in the future. Although Np Mössbauer spectroscopy has made important contributions in elucidating the bond structure in non-metallic compounds of neptunium (see, for example ref. 10 and references given therein), high pressure data for such materials do not exist.

2. Some experimental considerations

We have to assume that the reader is familiar with the basics of Mössbauer spectroscopy. An introduction with special emphasis on the case of actinide research can be found in ref. 7. The special technical features using ^{237}Np at ambient or elevated pressures are given in ref. 11, and details of the high pressure spectrometer can be found in ref. 12.

All measurements were performed with ^{241}Am metal as source (about 50 mCi) kept at 4.2 K (or lower). The compounds under investigation were used as absorbers and mounted inside a high pressure cell of the Bridgeman type using B_4C anvils. The rather large absorber area required (about 5 mm diameter) together with the necessary encapsulation for radiation safety (about 8 mm diameter) restricted the pressure range to no more than 9 GPa. Pressure loading is carried out at room temperature; the cell inside a high pressure clamp is then brought into a cryostat allowing measurements between 1.5 K and about 150 K. Pressure and pressure gradient are determined *in situ* with a manometer making use of the pressure dependence of the superconducting transition temperature of lead [13]. At $\langle P \rangle = 9$ GPa the gradient was found to be less than 5%.

Mössbauer spectroscopy is a nuclear counting experiment and as such is susceptible to counting statistics. A spectrum cannot be obtained instantaneously. In a high pressure measurement this requires counting times of several days.

Bulk moduli were obtained (preferentially at cryogenic temperatures) with a Guinier-type X-ray spectrometer and high pressure cells and clamps of basically similar design as those used in the Mössbauer measurements. The system is described in ref. 14.

3. Hyperfine interactions in neptunium

Information on electron structure by Mössbauer spectroscopy is based on the measurement of hyperfine interactions, that is the coupling of the electromagnetic moments of the nucleus with the fields produced by the surrounding electrons. In the case of Np it suffices to consider only the influence of its own electron shell which, however, is modified by the bonding to ligands. It is common practice to separate the hyperfine interaction experiment into three terms.

(i) The isomer shift arises from the Coulomb interaction of electronic charge density ρ_0 entering the nucleus (contact density) and the protonic charge distribution. Only s (and relativistic $p_{1/2}$) electrons contribute directly to ρ_0. However, the potential created by other electrons in the shell alters the orbits of s electrons and consequently their charge distribution which leads to an indirect influence on ρ_0. The presence of contact density produces a shift of the centre of gravity of the Mössbauer pattern away from zero velocity (between source and absorber). This is called the isomer shift S, measured in velocity units. One must refer S to an artificially chosen standard assigned $S = 0$. In case of ^{237}Np this is $NpAl_2$. Details on the theory of isomer shift can be found in ref. 15 and the situation in Np is dealt with extensively in ref. 7. It is difficult to evaluate S quantitatively, but general trends have been well established. Each charge state (Np^{3+} to Np^{7+}) is characterized by a certain range of isomer shifts. Covalent effects in non-conducting compounds cause a shift towards the next lower charge state. Conduction electrons in metallic materials induce shifts towards the next higher charge state. In the latter case volume reductions increase ρ_0 mainly via the compression of conduction electrons.

(ii) The quadrupole splitting is caused by the electric interaction between the non-spherical parts of the nuclear and the electronic charge distributions. The former is described by the nuclear quadrupole moment, the latter by the electric field gradient. For details we refer to ref. 7 or 8. Since quadrupolar effects are not discussed explicitly in this review we shall not pursue this term any further.

(iii) The nuclear Zeeman splitting results from the action of the magnetic field (the hyperfine field B_{hf}) produced by electrons in open shells on the magnetic dipole moment of the nucleus. This is the hyperfine term we are most concerned with. It leads to a multiline absorption spectrum of the kind shown in Fig. 1. More details are again to be found in ref. 7 and 8.

The magnitude of the hyperfine field can easily be extracted from the measured Zeeman pattern. As a first guess one may simply take the separation of the outermost spectral lines. The dominant source of B_{hf} in Np is the orbital motion of its 5 f electrons. This even holds for the cases of fairly wide 5 f bands in intermetallic compounds owing to relativistic effects [17]. For this reason B_{hf} is proportional to μ_{Np}, the magnetic moment resting on the neptunium ion. Experimentally the relation

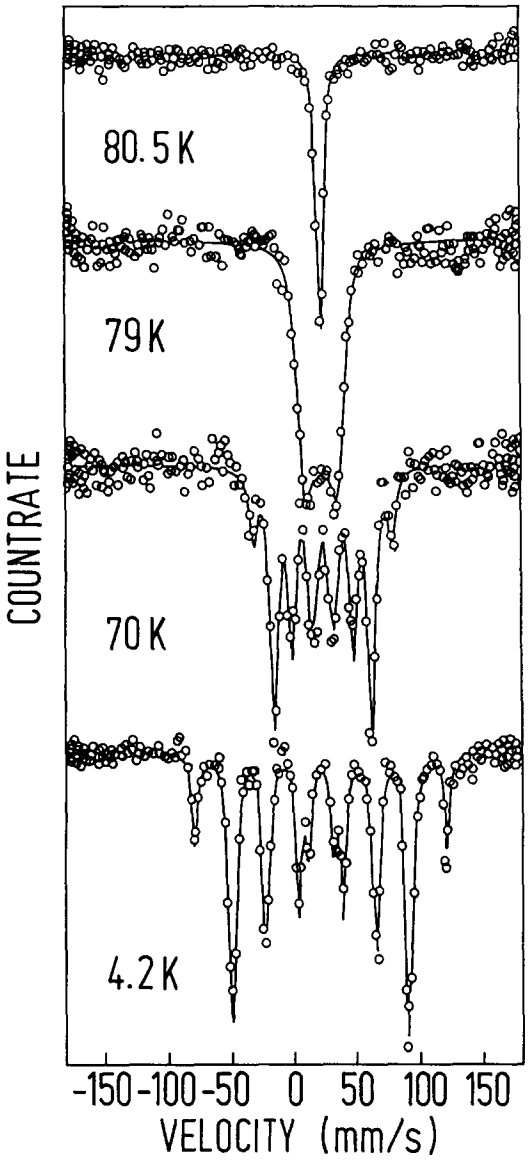

Fig. 1. Mössbauer spectra of antiferromagnetic Np_3As_4 at different temperatures. The magnetic transition occurs at 80 K. The spectrum at 4.2 K is the fully developed Zeeman pattern. After ref. 16.

$$\frac{B_{hf}}{\mu_{Np}} = 2150\text{kG}/\mu_B^{-1}$$

has been established over a wide range of fields and moments [18, 19]. Hence Mössbauer spectroscopy can be used for determining the magnetic moment on Np as well as its change with pressure.

The Zeeman splitting and with it the magnitude of B_{hf} in a magnetically ordered material is dependent on reduced temperature T/T_m where T_m is the temperature of onset of long-range order (Curie or Néel point). According to Fig. 1 the splitting diminishes with approach to T_m and vanishes above it, that is in the paramagnetic regime. The latter statement is not correct

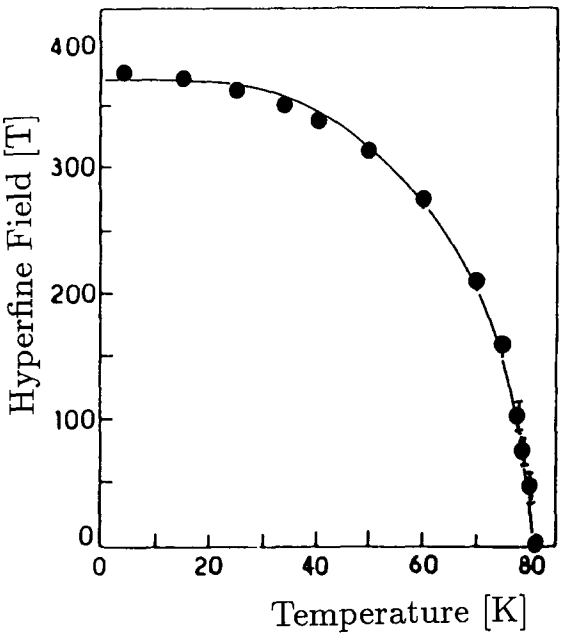

Fig. 2. Plot of effective hyperfine field *vs.* temperature as determined from Mössbauer spectra of the type shown in Fig. 1. Extrapolation to $T \to 0$ gives the saturation hyperfine field which is a measure of the moment on Np. Extrapolation to $B_{hf} \to 0$ gives the magnetic transition temperature T_m.

under all circumstances. Paramagnetic hyperfine spectra can be observed in certain cases [10]. However, in the compounds under discussion here, $B_{hf}(T)$ follows in the first approximation the temperature dependence of spontaneous (sublattice) magnetization $M(T)$. A typical example is presented in Fig. 2. The extrapolation of $B_{hf}(T) \to 0$ allows then the determination of the Curie or Néel temperature T_C or T_N respectively via Mössbauer spectroscopy. The relation between B_{hf} and μ_{Np} quoted above refers to the saturation hyperfine field, that is, to $B_{hf}(T \to 0)$.

In summary, we are able to measure $\Delta B_{hf}/\Delta P$ and $\Delta T_m/\Delta P$ as magnetic parameters. Combining these data with the bulk moduli leads to the volume coefficients $-\text{d ln } B_{hf}/\text{d ln } V \triangleq -\text{d ln } \mu_{Np}/\text{d ln } V$ and $-\text{d ln } T_m/\text{d ln } V$. From the observed change in isomer shift we further obtain $-\text{d ln } S/\text{d ln } V \triangleq -\text{d ln } \rho_0/\text{d ln } V$. These are the quantities we employ to gain insight into the volume dependence of the electronic structure properties of Np.

4. Delocalization of 5f electrons

The 5f electron structure in Np intermetallics can be described by 5f bands of varying width. Hence the magnetic properties of those compounds can vary from localized 4f-like (narrow band) to 3d-like itinerant electron (wide band) behaviour. Of course, a simple

comparison with the 4f or 3d transition series has to be taken with some care since spin–orbit coupling and other relativistic effects on electron properties are always more enhanced in the actinide series. As we shall show, high pressure Mössbauer data give important information with respect to 5f delocalization.

Figure 3 demonstrates the great variation in changes in hyperfine field (magnetic moment) with pressure-induced change in Np–Np separation d_{Np} in different intermetallic compounds. Except for the variation in hyperfine field in $NpOs_2$ the dependences are to a good approximation linear and allow easily the determination of the volume coefficients $-\mathrm{d}\ln B_{hf}/\mathrm{d}\ln V$ etc. For $NpOs_2$ the average slope was taken. The volume coefficients are summarized in Table 1. High pressure Mössbauer data also exist for $NpGa_3$ and $NpIn_3$ and will be discussed below. However, the bulk moduli are not available at this stage and hence they cannot be

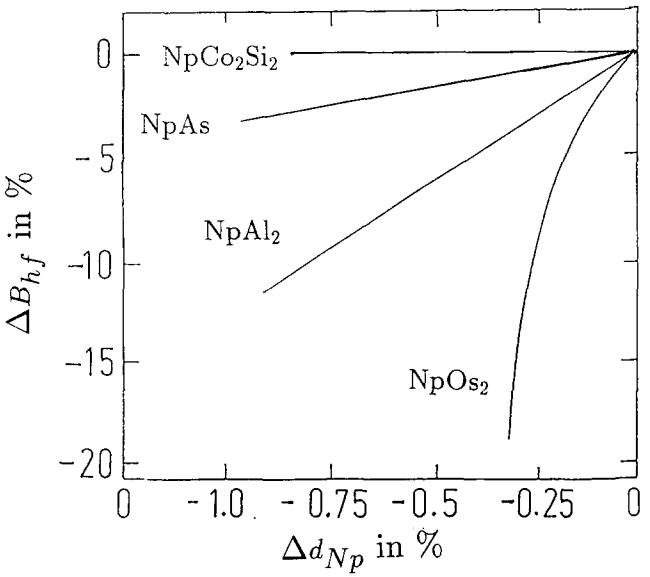

Fig. 3. Dependence of hyperfine field of several Np intermetallics on the reduction in the Np–Np separation d_{Np} as induced by the application of external pressure.

TABLE 1. Volume coefficients of the magnetic ordering temperature T_m, the ordered magnetic moment μ_{Np}, the electronic contact density $\rho(0)$ and the Np–Np separation d_{Np}

Compound	$\frac{-\mathrm{d}\ln T_m}{\mathrm{d}\ln V}$	$\frac{-\mathrm{d}\ln \mu_{Np}}{\mathrm{d}\ln V}$	$\frac{-\mathrm{d}\ln \rho(0)}{\mathrm{d}\ln V}$	d_{Np} (Å)
$DyAl_2$	+5.3	+0.1	$+5.6\times10^{-5}$	
UN	−19	−19		
$NpCo_2Si_2$	+3.3	+0.1	$+2.4\times10^{-5}$	3.90
NpAs	−1.3	−0.8	$+4.2\times10^{-5}$	4.07
$NpAl_2$	−16.0	−0.4	$+5.0\times10^{-5}$	3.37
$NpOs_2$	−80.0	−46.0	$+12.5\times10^{-5}$	3.28
$NpSn_3$	+8.0	$\leqslant +1.0$	$+2.0\times10^{-5}$	4.62

included in the table. Also presented are results for $DyAl_2$ which serves as a standard for a highly localized f electron configuration and UN which is considered a strongly itinerant electron antiferromagnet. The $DyAl_2$ data come from Mössbauer studies [20] while the coefficients for UN have been obtained by neutron and magnetization measurements [21, 22]. For a localized f electron magnet one expects the magnetic moment to be rather independent of volume (and close to the free ion value) while the magnetic transition temperature should sharply rise with reduced volume as predicted within the framework of the Ruderman–Kittel–Kasuya–Yoshida (RKKY) model (for a recent discussion and pertinent references see, for example, [23]). $DyAl_2$ exhibits these features. Itinerant electron magnets, in contrast, will have large reduction with decreasing volume of both the magnetic moment (hyperfine field) and the transition temperature. This is well borne out by the example of UN. For this material the pressure effect on magnetic properties has recently been discussed in terms of energy band calculations within the local spin density approximation [24]. It was found that the moment decrease is more pronounced for an antiferromagnetic than a ferromagnetic ground state, but the calculated value falls short by nearly a factor of 5 with respect to the measured value.

Let us discuss first the Laves phase materials. Within this series d_{Np} crosses the Hill limit (see also Fig. 4). The volume coefficients of magnetic moment and transition temperature exhibit for both $NpAl_2$ and $NpOs_2$ the behaviour expected for delocalized 5f electrons, the delocalization being much weaker in $NpAl_2$ than in $NpOs_2$ which lies close to the Hill limit. $NpOs_2$ is the most strongly itinerant Np intermetallic found thus far. We have already remarked on the non-linear dependence of $B_{hf}(P)$. The same behaviour is observed for $S(P)$ meaning that the correlation between B_{hf} and S remains linear and that the non-linear volume dependences of these two parameters directly reflect a non-linear change in electron structure. Band structure calculations not being available we cannot pinpoint the origin of this effect. Figure 4 demonstrates that the variation in hyperfine parameters with change of ligand is dominated by volume effects. These NpX_2 compounds are thus models for Hill-type behaviour, meaning that 5f–5f overlap is the decisive mechanism for 5f delocalization. This straightforward behaviour, however, is lost when 3d ligands are involved [8, 25] (*i.e.* $NpMn_2$, $NpFe_2$, $NpNi_2$, $NpCo_2$). Although high pressure data do not exist, hyperfine fields and isomer shift do not correlate any longer with d_{Np}. Hybridization with 3d electrons clearly comes into play [26]. Their magnetic behaviour, especially that of $NpCo_2$ [27], is also poorly understood at this stage.

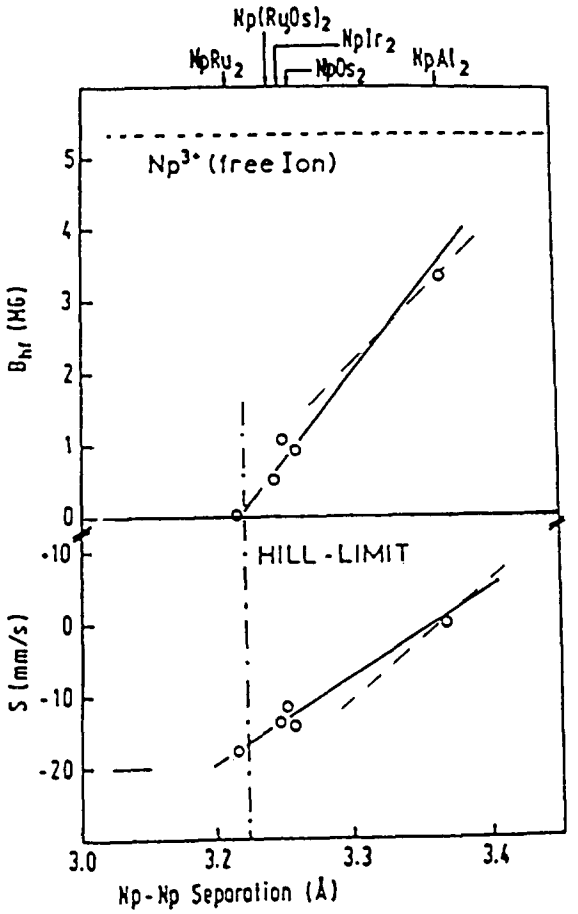

Fig. 4. Hyperfine fields and isomer shifts for cubic Laves phases NpX_2 (excluding 3d elements as ligands) against the separation d_{Np} of neptunium ions. – – –, pressure-induced variations in B_{hf} and S for $NpAl_2$.

Although d_{Np} in the NaCl-type NpX compounds is well above the Hill limit, simple localized 4f-like properties are not observed. High pressure data on NpAs indicate weakly delocalized behaviour (Table 1), and a plot of B_{hf} or S *vs.* lattice constant for different ligands still reveals a definite volume dependence which, however, is not the same for X≡chalcogenide and X≡pnictide. The latter fact demonstrates that the chemical nature of the ligand is now of importance as well [8, 25]. Only NpBi (the most voluminous in the series) exhibits definite signs of 4f-like localization [28], but no proof by pressure data exists. Since d_{Np} in NpX intermetallics is too large for substantial 5f–5f overlap, the formation of (albeit narrow) 5f bands must be caused by hybridization with ligand p electrons. The electronic structure of this series has been thoroughly dealt with theoretically (for example, ref. 29) but volume-dependent calculations only exist for UN, as mentioned.

The NpX_3 series with the $AuCu_3$ structure displays little systematic behaviour. Several compounds (*e.g.* $NpRh_3$) exhibit no magnetism, despite d_{Np} being far above the Hill limit. Also, the variation in isomer shift spans a range larger than that expected for a single Np charge state. No simple relations of hyperfine parameters with volume exist [8, 25]. The compound with the most surprising features within this series is $NpSn_3$. It undergoes magnetic order at 9.5 K basically into a type I antiferromagnetic structure but with a rather small moment (about $0.3\mu_B$). This, together with specific heat data, led to the assignment of $NpSn_3$ as a model itinerant electron antiferromagnet [30], a view supported at least in part by band structure calculations [31]. Consequently, one expected to find a high pressure behaviour similar to that of $NpOs_2$ but, as Fig. 3 and Table 1 demonstrate, the opposite was seen [32], namely the signature of a localized f electron structure. The unusual results were explained qualitatively by invoking the Kondo effect with a characteristic temperature $T^* \approx 30$ K [32] in analogy to the features of the well-established concentrated Kondo system $CeAl_2$ [33].

$NpIn_3$ differs only by one p electron when compared with $NpSn_3$ (and hence exhibits nearly the same isomer shift), yet its ambient magnetic features are quite different. It orders at higher temperatures (17 K) and its magnetic structure must be complex (see discussion in the next section). The maximum moment of $1.5\mu_B$ is rather normal for Np intermetallics. On the contrary, the changes in B_{hf} (or μ_{Np}) and T_N with pressure are quite alike in $NpSn_3$ and $NpIn_3$ [34].

The third member of the $AuCu_3$ system studied under high pressure is $NpGa_3$ [34]. We shall discuss this material mainly in the context of its magnetic phase diagram in the following section. The plots shown in Fig. 7 demonstrate that in this compound as well the influence of pressure on B_{hf} is minute but a substantial increase in the ordering temperature is induced. Most probably, the fairly similar pressure dependences for the three NpX_3 compounds just described reflect mainly their behaviour as Kondo lattice systems. The classification as Kondo systems is supported by resistivity measurements [35, 36].

The last candidate to be discussed is $NpCo_2Si_2$ [37] which also is the only non-cubic intermetallic measured under pressure. It crystallizes in the tetragonal (*I4/mmm*) structure and is a type I antiferromagnet with $T_N = 46$ K and $\mu_{Np} = 1.3\mu_B$ at ambient pressure. According to Table 1 the volume coefficients of μ_{Np} and T_N prove $NpCo_2Si_2$ to be the most localized compound studied thus far.

The volume dependence of isomer shift S (or contact density ρ_0) varies comparatively little between the various compounds. It largely reflects the compressibility of conduction electrons. As expected, it is largest for itinerant electron structures, in particular $NpOs_2$. The pressure dependence of isomer shift leads us, however, to another special magnetic feature for the cases of 4f-like localized antiferromagnets. Within the RKKY

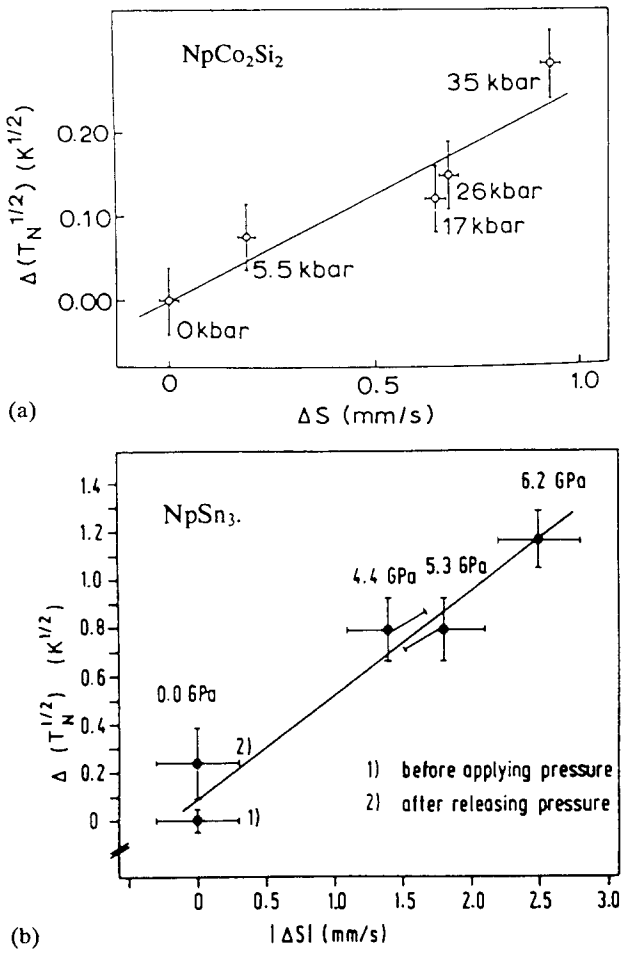

Fig. 5. Change in $T_N^{1/2}$ *vs.* change in isomer shift at various pressures for (a) $NpCo_2Si_2$ and (b) $NpSn_3$ (1 GPa≙10 kbar). The fulfilment of the relation $\Delta T_N^{1/2} \alpha \Delta S$ is independent proof of a localized 5f electron configuration.

model one may derive for the Néel temperature a relation of the kind [23].

$$T_N = C(\langle S_Z \rangle_{ce})^2$$

where C contains quantities (such as the Fermi energy) which are little (if at all) dependent on volume. $\langle S_Z \rangle_{ce}$ represents the effective conduction electron polarization. It is reasonable to assume that its change with volume is reflected in the compression of conduction electrons revealed by $S(P)$. Hence we expect that under pressure the relation $\Delta T_N^{1/2} \alpha \Delta S$ will hold. Figure 5 shows the results for $NpCo_2Si_2$ and $NpSn_3$ which independently establish the localized 5f electron structure in these compounds.

5. Magnetic phase diagrams

Especially in antiferromagnets of the light actinides the observed spin structure often results from a delicate balance between different interactions such as exchange, anisotropy and quadrupolar couplings. One observes dramatic changes in spin structure not only with temperature or applied field but also with reduced volume. Volume is a parameter which in principle can be handled more easily theoretically than temperature and hence the magnetic P–T phase diagram should be highly useful in analysing the interactions driving magnetic order. Mössbauer spectroscopy cannot give direct information on the spin structure, unlike neutron diffraction. However, the presence of complex antiferromagnetic arrangements such as modulated structures is well reflected in the Mössbauer spectrum via a distribution in hyperfine fields.

The first case to be discussed is NpAs. Neutron data [38] reveal that at ambient pressure a sinusoidally modulated incommensurate antiferromagnetic spin structure is formed below $T_N = 173$ K. At 153 K the modulation squares up and locks into a 4 up–4 down sequence. The magnetic ground state is a type I noncollinear (3 k) up–down structure which exists below 138 K. The various magnetic transitions are reflected in the Mössbauer spectra [39]. In particular, the change at 138 K is signalled by a sudden increase in B_{hf} of about 10%. Neutrons see a similar increase in moment. Figure 6 presents the pressure dependence of B_{hf} at

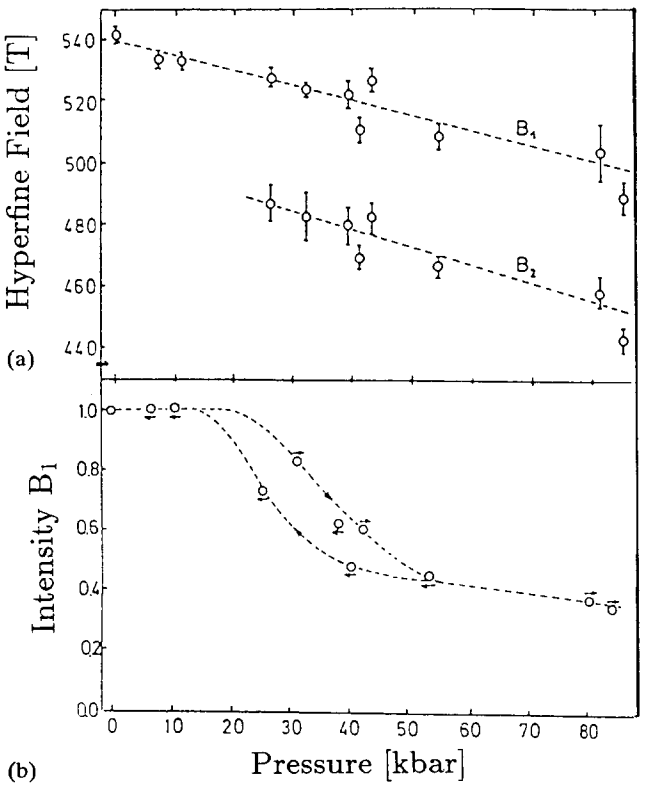

Fig. 6. (a) Variation in hyperfine field with pressure at 4.2 K in NpAs. At about 20 kbar (2 GPa) a second hyperfine pattern (B_2) appears. (b) The intensity of the first pattern (B_1) diminishes with pressure in favour of B_2.

4.2 K. Above about 2 GPa a second hyperfine spectrum with about 10% smaller B_{hf} appears. It becomes increasingly intense with rising pressure. Tentatively (*i.e.* in the absence of additional magnetic data) we give the following explanation. At ambient pressure the unit cell volume in the range of existence of the non-collinear up–down structure ($T<138$ K) is larger and B_{hf} bigger by about 10% than in the range of the collinear 4 up–4 down structure ($T\approx 140$ K) [40]. Reduction of volume by applied pressure favours even at low temperatures the formation of a collinear structure (probably the 4 up–4 down sequence) which is signalled by the appearance of the lower B_{hf}. The transition into the high pressure magnetic phase is sluggish, exhibits hysteresis and is incomplete within the pressure range covered.

In $NpGa_3$ at ambient pressure antiferromagnetic order sets in at 65 ± 2 K. Around 50 K a first-order transition into ferromagnetism occurs. The saturation hyperfine field corresponds to $\mu_{Np}=1.56\mu_B$ [35, 41]. Measurements of $B_{hf}(T)$ are depicted in Fig. 7 [42]. The Curie point is represented by the onset of magnetic splitting and the first-order Néel point by a discontinuous change in B_{hf} (see the 0 GPa data of Fig. 7). As is typical for a first-order transition the ferro- and antiferromagnetic phases coexist over a certain temperature range. Bouillet *et al.* [35] constructed from additional magnetization data the *B–T* phase diagram at ambient pressure given in Fig. 8(a). From Fig. 7 we learn that already at pressures of less than 3.5 GPa the discontinuity in $B_{hf}(T)$ disappears, meaning that at elevated pressures ferromagnetic alignment of spins is enforced beginning right at the transition into ordered magnetism. This leads us to propose the *P–T* phase diagram presented in Fig. 8(b). In summary, a suppression of the antiferromagnetic phase can be achieved either by applied fields in excess of 40 kG or by pressure.

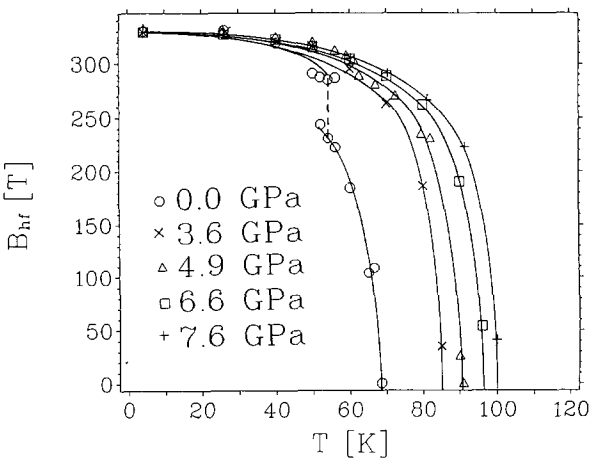

Fig. 7. Hyperfine field in $NpGa_3$ as function of temperature at different pressures.

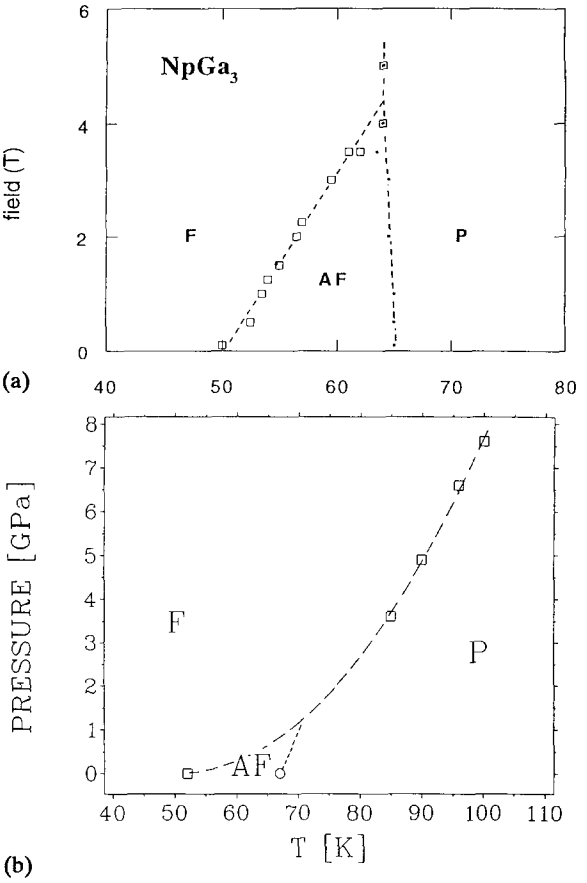

Fig. 8. Magnetic phase diagrams of $NpGa_3$ (F, ferromagnetic; AF, antiferromagnetic; P, paramagnetic): (a) *B–T* diagram after ref. 35; (b) *P–T* diagram [42].

Since single magnetic hyperfine patterns are observed throughout the pressure–temperature field covered (except in the region of the first-order transition at ambient and low pressures), we deal with simple ferro- and antiferromagnetic (*e.g.* type I) spin structures.

The situation in $NpIn_3$ is considerably more complex. Mössbauer spectroscopy and magnetization measurements cannot give any definite answers. Clearly, single-crystal neutron diffraction data are needed. In addition, it appears that details of the magnetic behaviour of $NpIn_3$ might be sample dependent. Gal *et al.* [41] find the onset of magnetic splitting near 17 K and conclude from magnetization measurements that at this temperature antiferromagnetic ordering commences. In contrast, Charvolin [36] interprets (more extensive) magnetization and resistivity data in terms of a Curie point at 14 K and a Néel point close to 10 K. The Mössbauer spectra available from various researchers [34, 36, 41–43] are in reasonable agreement; differences exist mainly in the temperatures where the various spectral shapes appear. The spectra of $NpIn_3$ at all temperatures and pressures are characterized by a distribution in hyperfine fields. Consequently there must exist a distribution of moments on Np which points

toward a modulated spin structure. Figure 9 presents typical spectra at ambient pressure and different temperatures as well as spectra at low temperature and different pressures. Looking first at the temperature dependence one notices that the prominent feature is a reduction in spectral intensity at the centre with rising temperature, meaning that in the field distribution low hyperfine fields become more and more absent. This change in spectral shape is continuous and we find no evidence for a sharp phase transition around 10 K [42]. The persistence of a field distribution in $NpIn_3$ proves that, in contrast to $NpGa_3$, we do not deal with simple ferro- or antiferromagnetic structures at all. In particular, the "ferromagnetic" phase suggested by Charvolin [36] must be a canted antiferromagnet, a cone structure or a complex ferrimagnet. Surely it would be quite unusual for a magnet first to order into a simple ferromagnetic structure and then to develop a complex antiferromagnetic structure as ground state. The spectra at low temperature and different pressures show that the loss of small fields in the field distribution, that is of central spectral intensity, can be induced by pressure as well. If we take the absence of small fields as the signature of the "ferromagnetic" phase then, in analogy to $NpGa_3$, a reduction in volume favours ferromagnetic spin couplings.

In all other Np intermetallics studied under high pressure (see Table 1) a change in magnetic structure with reduced volume was not observed.

6. Crystalline field interactions

In Fig. 10 the Mössbauer spectra of $NpAl_2$ at 4.2 K as function of pressure are shown. Clearly visible is the reduction in overall splitting (*i.e.* the diminution of B_{hf}) with rising pressure. However, the spectral shape observed at elevated pressures cannot be explained by a reduction in B_{hf} alone. A comparison with Fig. 1 makes it clear that, for example, the strong absorption line near zero velocity is unaccounted for in such an approach. The basic model which explains the spectral shapes observed calls for the existence of at least two states with different magnetic moments separated in energy by a few Kelvin only [44]. The states are occupied in thermal equilibrium and the electron configuration of the Np ion fluctuates rapidly between these states. In this case, the resulting Mössbauer spectrum is not

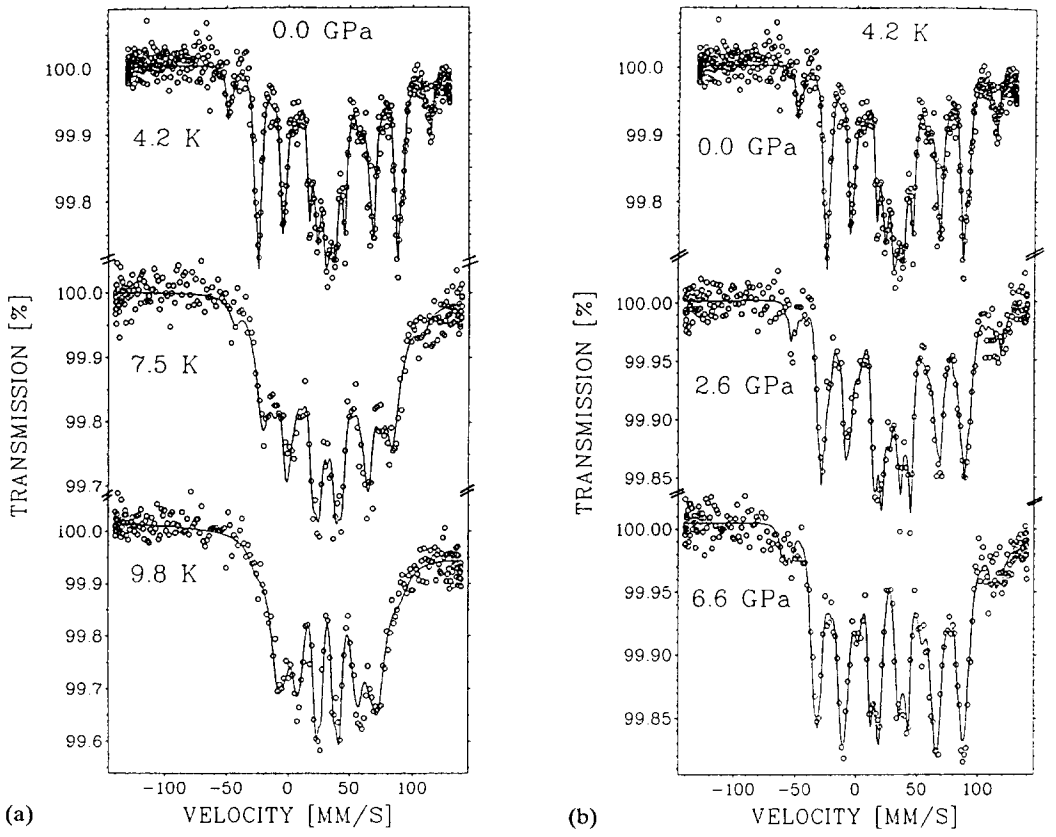

Fig. 9. Mössbauer spectra of $NpIn_3$ in the magnetically ordered regime (a) at ambient pressure and various temperatures and (b) at low temperature and various pressures. It should be noted that rising temperature and increasing pressure induce similar changes in spectral shape (neglecting the trivial reduction in hyperfine splitting with temperature: see Figs. 1 and 2).

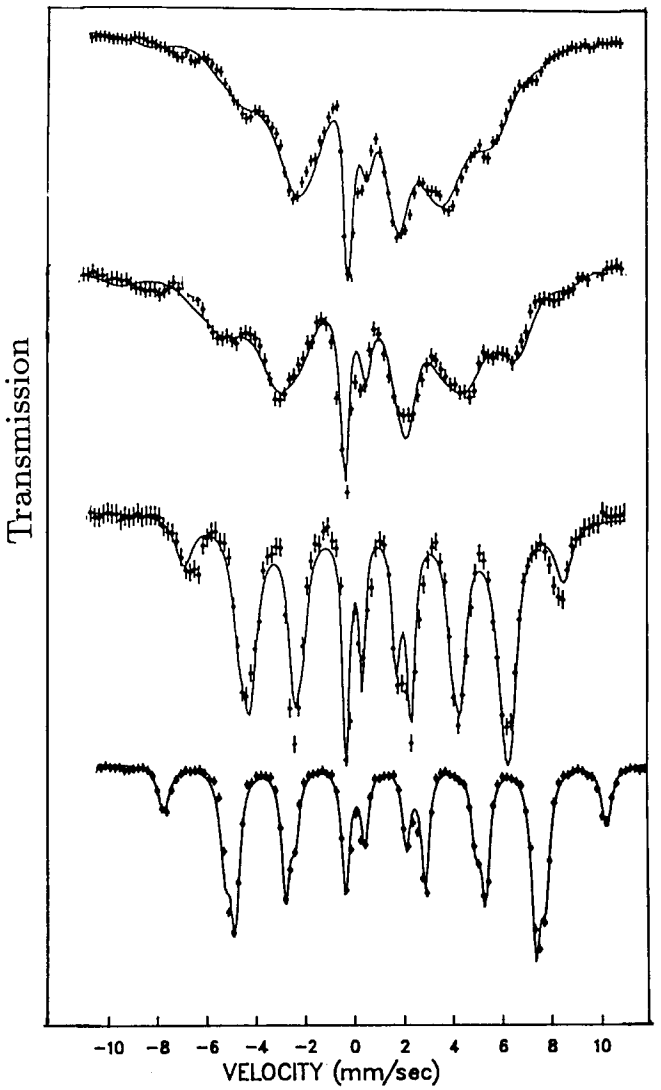

Fig. 10. Mössbauer spectra of $NpAl_2$ at 4.2 K and pressures of 0, 3.6, 7.2 and 9.0 GPa (bottom to top). ——, fit invoking crystalline electric field (CEF) states as discussed in the text.

simply the overlay of the patterns produced by the hyperfine parameters of the different states but a single pattern arising from dynamically averaging these various contributions. These types of spectra are known as "relaxation spectra" in the Mössbauer literature. Details concerning the case of Np can be found in ref. 7.

A crucial question is whether the different states involved produce the same isomer shift. If not, then we deal with a situation comparable with that in rare earth compounds with intermediate valence [45]. One then also expects a definite change in observed shift with temperature at constant pressure. This was not found in $NpAl_2$ and one concludes that the different states involved in producing the Mössbauer spectra of $NpAl_2$ shown in Fig. 10 must belong to the same formal charge state of Np. Recently we have succeeded [46] in explaining those spectra consistently with the help of CEF interactions [47]. We briefly outline the basic ingredients; a detailed discussion is beyond the scope of this review.

From the systematics of hyperfine parameters in Np intermetallics [8, 25] it has been argued that the formal charge state of Np in the NpX_2 compounds is Np^{3+}. Furthermore, the [001] direction is taken as the easy axis of magnetization. This makes the signs of the CEF parameters in $NpAl_2$ the same as those known for the RFe_2 compounds [48]. At ambient pressure the values of CEF parameters in the scheme of ref. 47 are such that one is near the cross-over between the Γ_5 and the Γ_6 levels. The different CEF states produce different values of B_{hf} (or μ_{Np}), as required, but the same ρ_0. The resulting Mössbauer spectra are calculated by dynamically averaging appropriately the interactions caused by the three lowest-lying CEF states in the cross-over regime mentioned. The effect of pressure is an increase in the ratio A_6/A_4 of the CEF parameters which causes drastic changes in the sequence and electronic properties of the CEF states and in turn in the hyperfine spectra produced by them. Unfortunately, the success of this approach as demonstrated by the fits shown in Fig. 10 is no definite proof for a Np^{3+} charge state, since an analogous cross-over region (Γ_6 to Γ_8) can be found in the CEF scheme of Np^{4+}. The important conclusion is that CEF interactions have to be taken into account even if the 5f electron configuration of the Np ion is not fully localized. Despite this fact, the CEF scheme developed for rare earth ions (*e.g.* ref. 47) works in good approximation.

In the $AuCu_3$ materials discussed earlier which behave in a well-localized manner under pressure, CEF interactions are likely to play an important role as well. However, alone they will not suffice. For example, the very low μ_{Np} in $NpSn_3$ cannot be produced in a CEF scheme.

The tetragonal systems NpX_2Si_2 or NpX_2Ge_2 have, if one generalizes the high pressure result of $NpCo_2Si_2$, highly localized 5f electrons and one expects CEF interactions to be dominant. Experimental evidence in this direction exists from behaviour at ambient pressure. It is discussed in ref. 8 extensively. The volume dependence in $NpCo_2Si_2$ would be consistent with an isolated (*i.e.* singly occupied) CEF state (Γ_5^1). In summary, it appears at this stage that CEF interactions are much more prominent in intermetallic compounds of neptunium when compared with their uranium counterparts, which reflects the generally higher tendency towards 5f localization for Np.

References

1 W.N. Millner (ed.), *Plutonium 1970 and Other Actinides*, American Institute of Mining and the Metals Society AME, Vols. 1 and 2, New York, 1970.

2 H.H. Hill, in W.N. Millner (ed.), *Plutonium 1970 and Other Actinides,* American Institute of Mining and the Metals Society AME, Vols. 1 and 2, New York, 1970, p. 2.
3 D.D. Koelling, A.J. Freeman and G.O. Arbman, in W.N. Millner (ed.), *Plutonium 1970 and Other Actinides,* American Institute of Mining and the Metals Society AME, Vols. 1 and 2, New York, 1970, p. 194.
4 S.-K. Chan and D.J. Lam, in W.N. Millner (ed.), *Plutonium 1970 and Other Actinides,* American Institute of Mining and the Metals Society AME, Vols. 1 and 2, New York, 1970, p. 219.
5 J.A. Stone and W.L. Pillinger, *Phys. Rev. Lett., 13* (1964) 200.
6 G.M. Kalvius, in W.N. Millner (ed.), *Plutonium 1970 and Other Actinides,* American Institute of Mining and the Metals Society AME, Vols. 1 and 2, New York, 1970, p. 296.
7 B.D. Dunlap and G.M. Kalvius, in A.J. Freeman and G.H. Lander (eds.), *Handbook on the Physics and Chemistry of Actinides,* Vol. 2, North-Holland, Amsterdam, 1985, p. 329.
8 W. Potzel, G.M. Kalvius and J. Gal, in K.A. Gschneidner, Jr., L. Eyring, G.H. Lander and G.R. Choppin (eds.), *Handbook on the Physics and Chemistry of Rare Earths,* Vol. 17, Elsevier, Amsterdam, 1993, p. 501.
9 J. Moser, J. Gal, W. Potzel, G. Wortmann, G.M. Kalvius, B.D. Dunlap, D.J. Lam and J.C. Spirlet, *Physica B, 102* (1980) 199.
10 G.M. Kalvius, *J. Less-Common Met., 121* (1986) 353.
11 W. Potzel, J. Moser, L. Asch and G.M. Kalvius, *Hyperfine Interact, 13* (1983) 175.
12 G.M. Kalvius, *High Pressure Res., 2* (1990) 315.
13 J. Willer and J. Moser, *J. Phys. E, 12* (1979) 886.
14 W. Potzel, *High Pressure Res., 2* (1990) 367.
15 B.D. Dunlap and G.M. Kalvius, in G.K. Shenoy and F.E. Wagner (eds.), *Mössbauer Isomer Shifts,* North-Holland, Amsterdam, 1978, p. 15.
16 G. Amoretti, M. Bogé, J.M. Fournier, A. Blaise and A. Wojakowski, *J. Magn. Magn. Mater., 66* (1987) 236.
17 B. Johansson, O. Eriksson, L. Nordström, L. Severin and M.S.S. Brooks, *Physica B, 172* (1991) 101.
18 B.D. Dunlap and G.H., Lander, *Phys. Rev. Lett., 33* (1974) 1046.
19 J.Gal, F.J. Litterst, W. Potzel, J. Moser, U. Potzel, S. Fredo, S. Tapuchi, G. Shani, J. Jove, A. Cousson, M. Pages and G.M. Kalvius, *Phys. Rev. Lett., 63* (1989) 2413.
20 A. Kratzer, U. Potzel, J. Moser, F.J. Litterst, W. Potzel and G.M. Kalvius, *J. Magn. Magn. Mater., 104–107* (1986) 25.
21 J.M. Fournier, J. Beille, A. Boeuf, C. Veltier and A. Wedgewood, *Physica B, 102* (1980) 282.
22 J.M. Fournier, J. Beille and C.H. de Novion, *J. Phys. (Paris), Colloq. C4, 40* (1979) 32.
23 A. Gleissner, W. Potzel, J. Moser and G.M. Kalvius, *Phys. Rev. Lett., 70* (1993) 2032.
24 M.S.S. Brooks, *Physica B, 190* (1993) 55.
25 G.M. Kalvius, J. Gal, L. Asch and W. Potzel, *Hyperfine Interact., 72* (1992) 77.
26 O. Eriksson, B. Johansson and M.S.S. Brooks, *Phys. Rev. B, 39* (1989) 1315.
27 J.P. Sanchez, B. Lebeck, M. Wulff, G.H. Lander, K. Tomala, K. Mattenberger, O. Vogt, A. Blaise, J. Rebizant, J.C. Spirlet and P.J. Brown, *J. Phys.: Condens. Matter, 4* (1992) 9423.
28 J.P. Sanchez, A. Blaise, M.N. Bouillet, F. Bourdarot, P. Burlet, J. Rossat-Mignod, J. Rebizant, J.C. Spirlet and O. Vogt, in *21emes Journées des Actinides,* Montechoro, 1991.
29 B.R. Cooper, R. Siemann, D. Yang, P. Thayamballi and A. Bannerjea, in A.J. Freeman and G.H. Lander (eds.), *Handbook on the Physics and Chemistry of Actinides,* Vol. 2, North-Holland, Amsterdam, 1985, p. 435.
30 R.J. Trainor, M.B. Brodsky, B.D. Dunlap and G.K. Shenoy, *Phys. Rev. Lett., 37* (1976) 1511.
31 M.R. Norman and D.D. Koelling, *Phys. Rev. B, 33* (1986) 3803.
32 G.M. Kalvius, S. Zwirner, U. Potzel, J. Moser, W. Potzel, F.J. Litterst, J. Gal, S. Fredo, I. Yaar and J.C. Spirlet, *Phys. Rev. Lett., 65* (1990) 2290.
33 B. Barbara, J.X. Boucherle, J.L. Buevoz, M.F. Rossignol and J. Schweizer, *Solid State Commun., 24* (1977) 481.
34 S. Zwirner, W. Potzel, J.C. Spirlet, J. Rebizant, J. Gal and G.M. Kalvius, *Physica B, 190* (1993) 107.
35 M.N. Bouillet, T. Charvolin, A. Blaise, P. Burlet, J.M. Fournier, J. Larroque and J.P. Sanchez, *J. Magn. Magn. Mater., 125* (1993) 113.
36 T. Charvolin, *Ph.D. Thesis*, Université Joseph Fourier, Grenoble, 1993.
37 W. Potzel, J. Moser, G.M. Kalvius, C.H. de Novion, J.C. Spirlet and J. Gal, *Phys. Rev. B, 24* (1981) 6762.
38 P. Burlet, S. Quézel, M. Kusnietz, D. Bonnisseau, J. Rossat-Mignod, J.C. Spirlet, J. Rebizant and O. Vogt, *J. Less-Common Met., 121* (1986) 325.
39 U. Potzel, J. Moser, W. Potzel, S. Zwirner, W. Schießl, F.J. Litterst, G.M. Kalvius, J. Gal, S. Fredo, S. Tapuchi and J.C. Spirlet, *Hyperfine Interact., 47* (1989) 399.
40 A.T. Aldred, B.D. Dunlap, A.R. Harvey, D.J. Law, G.H. Lauder and M.H. Mueller, *Phys. Rev. B, 9* (1974) 3766.
41 J. Gal, I. Yaar, S. Fredo, I. Halevy, W. Potzel, S. Zwirner and G.M. Kalvius, *Phys. Rev. B, 46* (1992) 5351.
42 S. Zwirner, *Ph.D. Thesis,* Technical University Munich, 1994.
43 M.N. Bouillet, *Ph.D. Thesis*, Université Joseph Fourier, Grenoble, 1993.
44 F.J. Litterst, J. Moser, W. Potzel, U. Potzel, G.M. Kalvius, L. Asch, J. Gal and J.C. Spirlet, *Physica B, 144* (1986) 41.
45 I. Nowik, *Hyperfine Interact., 13* (1983) 89.
46 I. Nowik, J. Gal, F.J. Litterst, W. Potzel, L. Asch, J. Moser, U. Potzel, G.M. Kalvius and J.C. Spirlet, unpublished results.
47 K.R. Lea, M.J.M. Leask and W.P. Wolf, *J. Phys. Chem. Solids, 23* (1962) 1381.
48 U. Atzmony, M.P. Dariel, E.R. Bauminger, D. Lebenbaum, I. Nowik and S. Ofer, *Phys. Rev. B, 7* (1973) 4220.